Chinese Chemical Letters 35 (2024) 109581

Contents lists available at ScienceDirect

Chinese Chemical Letters

journal homepage: www.elsevier.com/locate/cclet

Post-synthetic modifications of MOFs by different bolt ligands for controllable release of cargoes

Hao Wang[a,*], Meng-Qi Pan[a], Ya-Fei Wang[a], Chao Chen[a], Jian Xu[b,*], Yuan-Yuan Gao[c], Chuan-Song Qi[a], Wei Li[a], Xian-He Bu[b]

[a] College of New Materials and Chemical Engineering, Beijing Key Lab of Special Elastomeric Composite Materials, Beijing Institute of Petrochemical Technology, Beijing 102617, China
[b] School of Materials Science and Engineering, National Institute for Advanced Materials, TKL of Metal and Molecule-Based Material Chemistry, Nankai University, Tianjin 300350, China
[c] College of Chemical Engineering, Inner Mongolia University of Technology, Hohhot 010051, China

ARTICLE INFO

Article history:
Received 8 November 2023
Revised 2 January 2024
Accepted 24 January 2024
Available online 1 February 2024

Keywords:
Post-synthetic modifications
Metal-organic frameworks
Bolting ligand
Control release
Cargo

ABSTRACT

Post-synthetic modifications (PSM) have drawn great attention as a vigoroso tool to tune or enhance the performance of metal-organic frameworks (MOFs). However, the current PSM method usually have to sacrifice the porosity of MOFs to enrich their functionality, such as pore space partition (PSP) and post-synthetic elimination and insertion (PSE&I), causing a trade-off in this aspect. To address this issue, we herein propose a new PSM strategy of using the size-matching ligands as the bolts to lock MOFs' pores, which could be anchored onto open metal sites (OMSs) after guest loading through a stepwise manipulation. As a result, the loaded cargoes undergo a controlled releasing process with respect to different bolt ligands. Our proposed strategy provides a promising way to balance the functionality and porosity of MOFs.

Metal-organic frameworks (MOFs) with highly ordered extended structures held together by coordination bonds between metal ions/clusters and organic ligands have been developed as a burgeoning area of materials research in recent years [1–3]. Thanks to their high specific surface areas and permanent porosity, MOFs have great perspectives in myriad application fields, such as gas adsorption and separation [4–7], catalysis [8–11], sensing [12–14], and cargoes delivery [15–19]. Given the vast choices of metal nodes and organic linkers [20–22], this class of hybrid crystalline materials can be customized literally with almost infinite combinations, endowing excellent tunablity in pore structures and chemistry [23–26]. In practice, many deliberately designed MOFs are difficult to obtain *via* one-pot direct synthesis, partly due to strict restrictions on reaction conditions [27–29]. In this context, post-synthetic modification (PSM) is regarded as a complementary strategy to achieve the same goal by appending or substituting functionalized organic linkers, inorganic nodes or even guest molecules [30–32], imparting superior flexibility into MOF chemistry.

Currently, the PSM method evolves into several strategies for the specific modification of MOFs, including post-synthetic metal exchange (PSME), post-synthetic ligand exchange (PSLE), post-synthetic guest exchange (PSGE), pore space partition (PSP), and post-synthetic elimination and insertion (PSE&I) [33,34]. Comparatively, PSP or PSE&I has proved to be a more facile and feasible PSM method, as it could avoid the uncertainties in exchange reactions; in most cases, open metal sites (OMSs) are utilized to implement a directional ligand insertion. For example, Long *et al.* established a strategy of increasing low-pressure CO_2 adsorption selectivity and uptake by appending polyamines to the OMSs of a given MOF [35,36]. However, such PSM methods enrich the functionality of parent MOFs with the sacrifice of their porosity and pore volume, especially for rigid MOFs [37–39]. Therefore, how to mitigate the trade-off between functionality and porosity is an imperative task in the exploitation of MOFs by virtue of PSM. It is worth noting that there were different types of surface capping agents have been successfully incorporated onto the external surface of various MOFs to mitigate the trade-off phenomenon [40–42]. Nevertheless, the surface capping agents touch on the entire surface of MOFs with overdose effect, not precisely on the pores.

Inspired by our previous work regarding MOF-based crystalline capsules [43], we herein propose a new post-synthetic strategy of grafting specific ligands as a bolt deliberately onto the pore channels, which can introduce new functionality *via* PSM without compromising the porosity. For proof-of-concept, a new K-Zn-MOF,

* Corresponding authors.
E-mail addresses: wangh@bipt.edu.cn (H. Wang), jxu@nankai.edu.cn (J. Xu).

https://doi.org/10.1016/j.cclet.2024.109581
1001-8417/

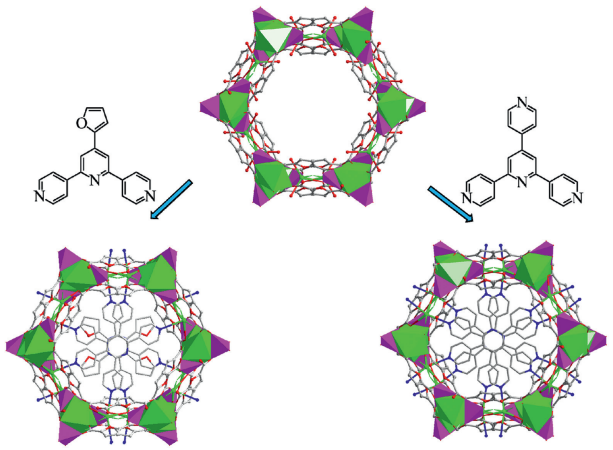

Fig. 1. Anchoring the size-matching bolt ligands onto the OMSs in the pore channel of **1** with one-pot solvothermal reaction.

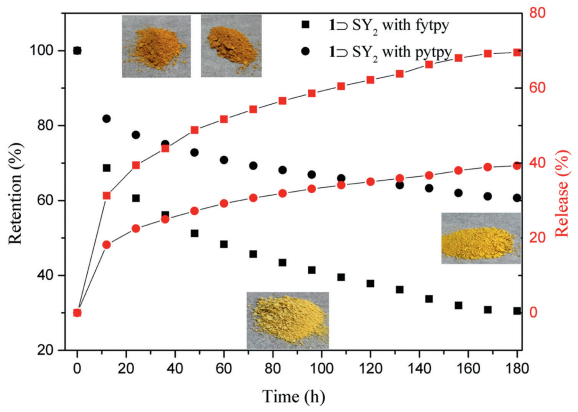

Fig. 2. Plots of the retention (left) and releasing (right) of **1**⊃SY_2 with different bolt ligands. Inset: photographs of the samples before and after cargo releasing.

$[K_2Zn(FDA)_2(H_2O)_2]$ (H_2FDA = 2,5-furandicarboxylic acid) (**1**) featuring one-dimensional channel enriched with OMSs was constructed. According to the size-matching rule, two organic ligands, 4′-(furan-2-yl)−4,2′:6′,4′′-terpyridine (fytpy) and 6′-(pyridin-4-yl)−4,2′:4′,4′′-terpyridine (pytpy), were selected and anchored into the MOF. The relevant experiments demonstrated that the introduction of different bolt ligands could effectively control the releasing of the loaded cargoes while not reducing their loading amount.

K-Zn-MOF (**1**) crystallizes in the rhombohedral space group $R\bar{3}c$ (Tables S1 and S2 in Supporting information) and possesses an isoreticular structure to Na-Zn-MOF with 1D neutral hexagonal channels [43]**.** The asymmetric unit consists of one-half crystallographically independent Zn^{2+} ions and two one-half K^+ ions (denoted as K1 and K2, respectively). K1 ions participate in the assembly of helical Zn-O-K-O rod-shaped units that were bridged by FDA^{2-} to form 1D hexagonal channels (Fig. S1 in Supporting information), while K2 ions coordinate with two water molecules (Fig. S2 in Supporting information), which can be removed upon activation to generate OMSs, evidenced by powder X-ray diffraction (PXRD) profiles and thermogravimetric analysis (TGA) of activated **1** (Figs. S3 and S4 in Supporting information). Without considering K^+ ions, the topology analysis shows that the whole framework of **1** can be simplified to a typical NbO topology (Fig. S5 in Supporting information). To verify whether the bolt ligands can be anchored onto the OMSs, one-pot solvothermal reaction similar to the synthesis of **1** was performed, with the addition of fytpy or pytpy ligand at the beginning of the reaction. Single crystal X-ray diffraction (SCXRD) analyses suggest the molecular formula of the resulting complexes **2** and **3** to be $[K_6Zn_3(fytpy)_2(FDA)_6]$ and $[K_6Zn_3(pytpy)_2(FDA)_6]$, respectively (Tables S1 and S2). As shown in Fig. 1, complexes **2** and **3** possess a similar three-dimensional (3D) framework as that of **1**, but with the fytpy or pytpy ligand embedded into the 1D channels by replacing the water ligands of K2 ions (Figs. S6 and S7 in Supporting information). The distinctive distribution of hetero atoms (i.e., N and O) in fytpy and pytpy ligand leads to a subtle difference between the structures of **2** and **3**. Specifically, the OMSs of K2 ions in **2** are two-thirds occupied by two N atoms from fytpy, while the rest OMSs are still retained due to the steric hindrance effect of furan ring. In contrast, the OMSs of K2 ions in **3** are all taken up by three N atoms from pytpy. Along with the trend in the occupied number of OMSs, the distance between the K2 ions accordingly decreases from 15.006 Å (for **1**), to 14.986 Å (for **2**) and 14.949 Å (for **3**). The inserted ligands are stacked in a face-to-face fashion by the π-π interactions between the adjacent ligands. The intermolecular distances between fytpy are 3.751, 4.532, and 3.760 Å, slightly longer than those of pytpy (3.731, 4.434, and 3.731 Å) (Fig. S8 in Supporting information). Due to the insertion of fytpy or pytpy, the whole unit cell volume of **2** or **3** is contracted compared with **1**. And **3** exhibits a higher thermal stability than that of **2** (Fig. S10 in Supporting information), likely ascribed to the full occupation of OMSs in **3**. All the above results demonstrate the feasibility of anchoring the size-matching ligands onto the OMSs in the pore channels.

For proof-of-concept of our proposed strategy, we carried out a stepwise process to investigate the "loading-bolting-releasing" of several cargoes (Scheme S1 in Supporting information) by different bolt ligands (fytpy and pytpy), including 4-dimethylaminoazobenzene (Solvent Yellow 2, SY_2), azobenzene (AB), 4-hydroxyazobenzene (HAB), 4-(phenylazo)benzoic acid (CAB), benzeneazo-2-naphthol (Solvent Yellow 14, SY_{14}), chlorambucil (CB, anticancer drug), methylene blue (MB^+), and fluorescein sodium (FS^-). In the releasing process, ethanol was selected as the medium for the stability of activated **1**. The detailed manipulation sequence is as follows (taking SY_2 as the example): Firstly, activated **1** was immersed in the ethanol solution of SY_2 for 24 h, followed by filtering to obtain the composite of **1**⊃SY_2. The loading capacity was around 6.9 wt% of activated **1,** indicated by UV–vis absorption spectroscopy and elemental analysis (EA). Secondly, the fytpy or pytpy ligand was mixed with **1**⊃SY_2 in the agate mortar. Thirdly, **1**⊃SY_2 bolted with fytpy or pytpy was soaked in ethanol, where the releasing of SY_2 was real-time monitored by UV–vis absorption spectroscopy.

Notably, the grafted fytpy and pytpy ligands exhibit distinctive bolting effect manifested in the color change before and after cargo releasing, which is distinguishable by the naked eyes. Before the releasing process, the initial color of **1**⊃SY_2 with fytpy is yellowish-brown, which is the same as that of **1**⊃SY_2 with pytpy (Fig. 2). After 180 h releasing, the color of **1**⊃SY_2 with fytpy faded to light yellow, while the color of **1**⊃SY_2 with pytpy turned to yellow (Fig. 2). The color changes of the two samples were consistent with their solid UV absorption spectra (Fig. S11 in Supporting information), by which the residual amount of SY_2 in **1**⊃SY_2 with fytpy was estimated to be *ca.* 30% after 180 h, while that of **1**⊃SY_2 with pytpy was as high as 60%. The similar phenomena were also observed when encapsulating different cargoes, such as AB, HAB, CAB, SY_{14}, and CB (Table S3 and Fig. S13 in Supporting information). All these results corroborated that pytpy exerts a much stronger bolting action on the pore channels of **1** than fytpy. This results in idiosyncratic controlling effects on the releasing of cargoes, as evidenced by the retention/releasing plots (Fig. S13), from which the bolting role of the inserted ligands is especially remark-

able for neutral molecules. In addition, the PXRD pattern of **1**⊃SY_2 with fytpy or pytpy, after 180 h releasing of SY_2, is nearly identical to the simulated profile of **1** (Fig. S14 in Supporting information), which suggests that the MOF could maintain its crystallinity throughout the "loading-bolting-releasing" process.

To investigate the mechanism of cargoes release, the release data were fitted by Korsmeyer–Peppas model [44–46], which reads as follows:

$$\left[\frac{M_t}{M_\infty}\right] = Kt^n$$

where M_t denotes the amount of cargo released at time t, M_∞ represents the total loaded amount of cargo, K refers to the release rate constant, and n is exponent constant, from which the release mechanism can be identified. According to the fitting results, the exponent constant n was estimated to be 0.29 and 0.28 for **1**⊃SY_2 with fytpy and pytpy, respectively, both of which can then be assigned to the Fickian diffusion mechanism ($n < 0.5$) [44–46]. In line with the color changes, there is a big discrepancy in their corresponding release rate constant K, which was 15.53 and 9.11, the former being about 1.7 times that of the latter. Both the diffusion mechanism and the trend of higher release rate constant for the MOF with fytpy ligand were kept when the cargoes were changed to AB, HAB, CAB, SY_{14}, and CB (Fig. S15 and Table S4 in Supporting information). Further, the bolt role of the ligands in the releasing process was investigated. As shown in Table S5 (Supporting information), the content of fytpy was declined along with the releasing process, while the content of pytpy was barely changed. This is likely attributed to the different coordination abilities of fytpy and pytpy ligands: there are two N atoms of fytpy coordinated to the OMSs in a line mode, while pytpy contributes three N atoms in a plane mode. Obviously, the pytpy linkage is more robust than fytpy, and such difference greatly influences the releasing rate of cargoes within the same release mechanism.

Except for neutral cargoes, the effect of bolt ligands on ionic guests (*e.g.*, cationic MB^+ and anionic FS^-) were also studied. The UV–vis absorption spectra showed that **1**⊃MB^+ with fytpy or pytpy can retain around 81% or 86% of MB^+ after 180 h releasing, while the residual amount of FS^- in **1**⊃FS^- with fytpy or pytpy was around 87% or 90% (Fig. S16 in Supporting information). Evidently, the two bolting ligands presented a marginal difference in controlling the releasing of ionic cargoes with respect to neutral ones. According to the fitting results, the release rate constants for MB^+ and FS^- were limitedly changed when fytpy ligand was replaced by pytpy (Fig. S17 in Supporting information). To figure out the reason behind this phenomenon, the zeta potential of activated **1** in ethanol was measured by a zeta potential analyzer (Fig. S18 in Supporting information). The value of −11.1 mV indicated the presence of negative surface charges, so that the ionic cargoes were adsorbed in **1** through electrostatic interactions, thereby making them difficult to release [47–50].

Considering the fact that the bolt ligand was anchored into the pore channel after the loading of guest molecules, the influence of the blots on the MOF porosity can be neglected. To testify this, we then measured the 77 K N_2 isotherms of activated **1** with and without the bolting ligands (Fig. 3). For the parent MOF **1**, the obtained type-I isotherm shows the N_2 adsorption capacity of 278 cm^3/g at 1 atm, from which the Brunauer-Emmett-Teller (BET) surface area was estimated to be 933 m^2/g. By using nonlocal density functional theory, the pore size distribution was calculated to be around 11 Å, in accordance with the value from SCXRD data. As we expected, the grafting of fytpy or pytpy ligand imposes a negligible influence on the porosity of **1**, as confirmed by the almost unchanged N_2 isotherms and pore size distribution (Fig. 3). It can be understood that the bolt ligands could substantially block the leaking of cargoes with large molecular size, but otherwise for the guests of small size, like N_2, which could freely pass through the gap between the bolt and the pore wall (Fig. S9 in Supporting information).

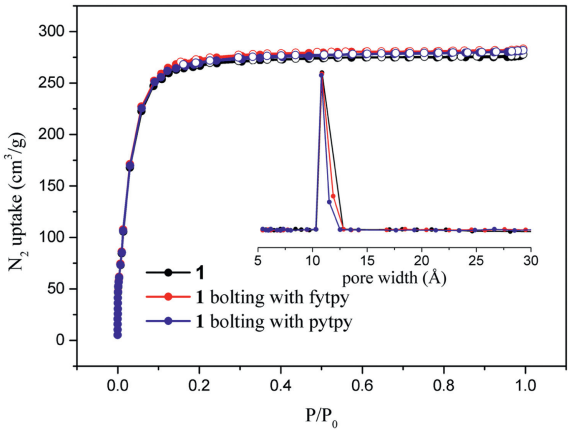

Fig. 3. N_2 adsorption-desorption isotherms of activated **1**, activated **1** bolting with fytpy and pytpy, respectively.

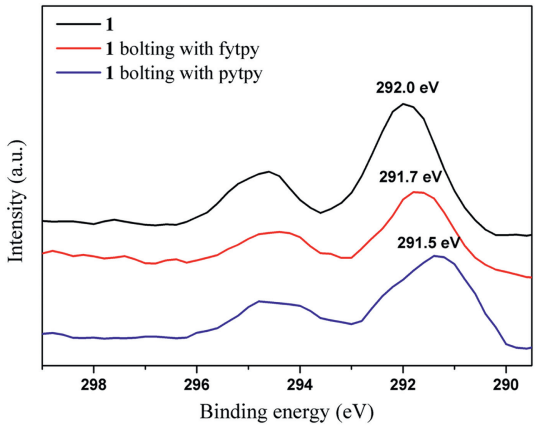

Fig. 4. A comparison of the binding energy of K $2p_{3/2}$.

As demonstrated above, OMSs are vitally important in the proposed strategy. To give deep insight into the role of OMSs, we conducted X-ray photoelectron spectroscopy (XPS) to study the chemical environment of K^+ ions in the MOF. The results showed that the intense peak for K $2p_{3/2}$ located at a binding energy (BE) of 292.0 eV in activated **1**, closer to that of K^+ ions [51–53]. With the increased N donor atoms in the bolt ligands, K^+ ions tend to be more electronegative with the BE values of 291.7 and 291.5 eV, indicative of a stronger interaction of K^+ ion with pytpy than fytpy (Fig. 4) [54,55]. It should be mentioned that one-pot synthesis of Na-Zn-MOF with fytpy failed after many trials. When changing Na^+ to K^+ ion, the K-Zn-MOF with fytpy ligand could be successful acquired, namely **2**. The reason was probably due to the larger radius of K^+ than Na^+, making K^+ ion easier to coordinate with fytpy.

In summary, we have presented a new post-synthetic strategy that mitigates the trade-off between functionality and porosity of MOFs with more precisely. A new 3D K-Zn-MOF with 1D channels enriched with potential OMSs was constructed. Two size-matching ligands, fytpy and pytpy, were selected and anchored onto the OMSs to serve as the bolts. The experimental results demonstrated that different bolting ligand can effectively tune the releasing rate of cargoes through a stepwise "loading-bolting-releasing" process, without compromising the porosity of the MOF. This strategy may shed new insights into the functionalization of MOFs *via* the post-synthetic modification.

Declaration of competing interest

The authors declare that they have no known competing financial interests or personal relationships that could have appeared to influence the work reported in this paper.

Acknowledgments

This work was financially supported by Natural Science Foundation of Beijing, China (No. 2212006), National Natural Science Foundation of China (Nos. 22171144, 21501012, 21806011 and 21761026), the Fundamental Research Funds for the Central Universities (Nankai University) and High-level Teachers in Beijing Municipal Universities in the Period of 13th Five–year Plan (No. CIT&TCD201904044).

Supplementary materials

Supplementary material associated with this article can be found, in the online version, at doi:10.1016/j.cclet.2024.109581.

References

[1] B.E.R. Snyder, A.B. Turkiewicz, H. Furukawa, et al., Nature 613 (2023) 287–291.
[2] L. Gagliardi, O.M. Yaghi, Chem. Mater. 35 (2023) 5711–5712.
[3] Y. Zhao, Y.H. Chai, T. Chen, et al., Chin. Chem. Lett. 35 (2024) 109298.
[4] X.B. Mu, Y.Y. Xue, M.C. Hu, et al., Chin. Chem. Lett. 34 (2023) 107296.
[5] W. Gong, Y. Xie, X. Wang, et al., J. Am. Chem. Soc. 145 (2023) 2679–2689.
[6] S.B. Geng, H. Xu, C.S. Cao, et al., Angew. Chem. Int. Ed. 62 (2023) e202305390.
[7] Z.M. Ye, X.F. Zhang, D.X. Liu, et al., Sci. China Chem. 65 (2022) 1552–1558.
[8] Y. Zhang, S. Chen, A.M. Al-Enizi, et al., Angew. Chem. Int. Ed. 62 (2023) e202213399.
[9] C.Q. Zhang, L. Yuan, C. Liu, et al., J. Am. Chem. Soc. 145 (2023) 7791–7799.
[10] S.Y. Wang, Z.W. Ai, X.W. Niu, et al., Adv. Mater. 35 (2023) 2302512.
[11] Q.B. Shen, J.L. Chen, X. Jing, C.Y. Duan, ACS Catal. 13 (2023) 9969–9978.
[12] S.L. Liu, J.T. Zhou, X. Yuan, et al., Food Chem. 432 (2024) 137272.
[13] K.X. Ma, J. Li, H.Y. Ma, et al., Chin. Chem. Lett. 34 (2023) 108227.
[14] S. Liu, Y.P. Huo, G.H. Li, et al., Chem. Eng. J. 469 (2023) 144027.
[15] a) X. Wang, L. He, J. Sumner, et al., Nat. Commun. 14 (2023) 973.
[16] K.Y. Wang, J.Q. Zhang, Y.C. Hsu, et al., Chem. Rev. 123 (2023) 5347–5420.
[17] C.B. Zhao, Z. Jiang, Y. Liu, et al., J. Am. Chem. Soc. 144 (2022) 23560–23571.
[18] R. Ou, H. Zhang, C. Zhao, et al., Chem. Mater. 32 (2020) 10621–10627.
[19] Y. Yang, G. Ren, W. Yang, et al., ACS Appl. Nano Mater. 4 (2021) 7191–7198.
[20] F. Xiang, H. Zhang, Y. Yang, et al., Angew. Chem. Int. Ed. 62 (2023) e202300638.
[21] P. Gao, K. Zhang, D. Ren, et al., Adv. Fun. Mater. 33 (2023) 2300105.
[22] N. Yu, M. Li, X. Chen, et al., ACS Appl. Energy Mater. 6 (2023) 12048–12051.
[23] X.L. Zhuang, S.T. Zhang, Y.J. Tang, et al., Coord. Chem. Rev. 490 (2023) 215208.
[24] Z. Zheng, H.L. Nguyen, N. Hanikel, et al., Nat. Protoc. 18 (2023) 136–156.
[25] Q.S. Cheng, Q. Ma, H.B. Pei, et al., Coord. Chem. Rev. 484 (2023) 215120.
[26] C. Dong, J.J. Yang, L.H. Xie, et al., Nat. Commun. 13 (2022) 4991.
[27] K.Y. Wang, Z.T. Yang, J.Q. Zhang, et al., Nat. Protoc. 18 (2023) 604–625.
[28] P. Sekar, P. Vasanthakumar, R. Shanmugam, et al., Green Chem. 24 (2022) 9233–9244.
[29] T.Y. Luo, S. Park, T.H. Chen, et al., Angew. Chem. Int. Ed. 61 (2022) e202209034.
[30] Y.C. Xiao, Y.C. Chen, A.N. Hong, X.H. Bu, P.Y. Feng, Angew. Chem. Int. Ed. 62 (2023) e202300721.
[31] T. Chen, D. Zhao, Coord. Chem. Rev. 491 (2023) 215259.
[32] M. Kalaj, S.M. Cohen, ACS Cent. Sci. 6 (2020) 1046–1057.
[33] S. Mandal, S. Natarajan, P. Mani, A. Pankajakshan, Adv. Fun. Mater. 31 (2021) 2006291.
[34] Z. Yin, S. Wan, J. Yang, M. Kurmoo, M.H. Zeng, Coord. Chem. Rev. 378 (2019) 500–512.
[35] B. Dinakar, A.C. Forse, H.Z.H. Jiang, et al., J. Am. Chem. Soc. 143 (2021) 15258–15270.
[36] E.J. Kim, R.L. Siegelman, H.Z.H. Jiang, et al., Science 369 (2020) 392–396.
[37] Z. Zhou, Q. Ke, M. Wu, L. Zhang, K. Jiang, ACS Mater. Lett. 5 (2023) 466–472.
[38] C.X. Chen, Z.W. Wei, T. Pham, et al., Angew. Chem. Int. Ed. 60 (2021) 9680–9685.
[39] Q.G. Zhai, X.H. Bu, X. Zhao, D.S. Li, P.Y. Feng, Acc. Chem. Res. 50 (2017) 407–417.
[40] Y. Liang, X. Yang, X. Wang, et al., Nat. Commun. 14 (2023) 5223.
[41] D. Wang, S. Li, C. Wu, T. Li, J. Am. Chem. Soc. 144 (2022) 685–689.
[42] J. Liang, V. Gvilava, C. Jansen, et al., Angew. Chem. Int. Ed. 60 (2021) 15365–15370.
[43] H. Wang, J. Xu, D.S. Zhang, et al., Angew. Chem. Int. Ed. 54 (2015) 5966–5970.
[44] a) H. Wang, T.L. Hu, R.M. Wen, Q. Wang, X.H. Bu, J. Mater. Chem. B 1 (2013) 3879–3882.
[45] V. Uskokovic, J. Mater. Chem. B 7 (2019) 3982–3992.
[46] T. Lu, T.L.M. TenHagen, J. Control. Release 324 (2020) 669–678.
[47] N.M. Mahmoodi, M. Oveisi, A. Taghizadeh, M. Taghizadeh, J. Hazard. Mater. 368 (2019) 746–759.
[48] H. Molavi, A. Hakimian, A. Shojaei, M. Raeiszadeh, Appl. Surf. Sci. 445 (2018) 424–436.
[49] C.X. Yu, Z.C. Shao, H.W. Hou, Chem. Sci. 8 (2017) 7611–7619.
[50] S.Q. Deng, X.J. Mo, S.R. Zheng, et al., Inorg. Chem. 58 (2019) 2899–2909.
[51] A. Ihs, K. Uvdal, B. Liedberg, Langmuir 9 (1993) 733–739.
[52] K.Y. Chun, C.J. Lee, J. Phys. Chem. C 112 (2008) 4492–4497.
[53] G.C. Allen, M.T. Curtis, A.J. Hooper, P.M. Tucker, J. Chem. Soc. Dalton Trans. (1973) 1675–1683.
[54] A.E. Baumann, X. Han, M.M. Butala, V.S. Thoi, J. Am. Chem. Soc. 141 (2019) 17891–17899.
[55] R.A. Peralta, M.T. Huxley, J.D. Evans, et al., J. Am. Chem. Soc. 142 (2020) 13533–13543.